Detection and monitoring of early airway injury effects of half-mustard (2-chloroethylethylsulfide) exposure using high-resolution optical coherence tomography

Kelly A. Kreuter
Sari B. Mahon
David S. Mukai
University of California, Irvine
Beckman Laser Institute
Irvine, California 92612
    and
University of California, Irvine Medical Center
Pulmonary and Critical Care Division
Orange, California 92868

Jianping Su
Woong-Gyu Jung
University of California, Irvine
Beckman Laser Institute
Irvine, California 92612
    and
University of California, Irvine
Department of Biomedical Engineering
Irvine, California 92697

Navneet Narula
University of California, Irvine Medical Center
Department of Pathology
Orange, California 92868

Shuguang Guo
Nicole Wakida
University of California, Irvine
Beckman Laser Institute
Irvine, California 92612

Chris Raub
University of California, Irvine
Department of Biomedical Engineering
Irvine, California 92697

Michael W. Berns
University of California, Irvine
Beckman Laser Institute
Irvine, California 92612

Steven C. George
Zhongping Chen
University of California, Irvine
Department of Biomedical Engineering
Irvine, California 92697

Matthew Brenner
University of California, Irvine
Beckman Laser Institute
Irvine, California 92612
    and
University of California, Irvine Medical Center
Pulmonary and Critical Care Division
Orange, California 92868

Abstract. Optical coherence tomography (OCT) is a non-invasive, high-resolution imaging technology capable of delivering real-time, near-histologic images of tissues. Mustard gas is a vesicant-blistering agent that can cause severe and lethal damage to airway and lungs. The ability to detect and assess airway injury in the clinical setting of mustard exposure is currently limited. The purpose of this study is to assess the ability to detect and monitor progression of half-mustard [2-chloroethylethylsulfide (CEES)] airway injuries with OCT techniques. A ventilated rabbit mustard exposure airway injury model is developed. A flexible fiber optic OCT probe is introduced into the distal trachea to image airway epithelium and mucosa *in vivo*. Progression of airway injury is observed over eight hours with OCT using a prototype time-domain superluminescent diode OCT system. OCT tracheal images from CEES exposed animals are compared to control rabbits for airway mucosal thickening and other changes. OCT detects the early occurrence and progression of dramatic changes in the experimental group after exposure to CEES. Histology and immunofluorescence staining confirms this finding. OCT has the potential to be a high resolution imaging modality capable of detecting, assessing, and monitoring treatment for airway injury following mustard vesicant agent exposures. © *2009 Society of Photo-Optical Instrumentation Engineers.* [DOI: 10.1117/1.3210775]

Keywords: optical coherence tomography; mustard gas; always injury.

1 Introduction

Sulfur mustard (SM) is a blistering agent and vesicant that was first synthesized in the 1800's and used extensively by the German army during World War 1 as a chemical warfare agent. It has been used in more than ten conflicts worldwide since, including the Iran-Iraq war in the late 1980's.[1–9] While sulfur mustard is no longer a conventional weapon during war, it continues to be a significant threat from developing

Address correspondence to: Matt Brenner, M.D., Professor of Medicine, Pulmonary and Critical Care Division, UC Irvine Medical Center, Bldg. 53, Rm 119, 101 City Drive South, Orange, CA 92868; Tel: 714 456-5150; Fax: 714 456-8349

nations and potential terrorists due to the ease of obtaining the components for production, the simplicity of production, the low cost, and the ease of concealment.[10] Massive stockpiles of mustard have been stored, buried, disposed of at sea, or are decaying in storage facilities worldwide that may pose the greatest potential threat as an environmental hazard at this time.[11]

Numerous physiological complications result from exposure to SM. The cellular complications resulting from exposure are thought to be mediated by the alkylation of DNA, which leads to breakage of the helical structure and crosslinking of DNA, RNA, and proteins, resulting in cellular apoptosis and effects on the cytoskeleton (specifically, actin).[11–13] Because these changes are occurring at a cellular level, the pathophysiologic effects resulting from exposure may not be apparent for up to 48 h following exposure.

Most commonly, the effects resulting from mustard exposure are respiratory, ocular, and cutaneous, though once the vesicant is absorbed into the body, it may affect entire internal organ systems. In addition to the immediate onset of blistering, there are intermediate pulmonary complications of suppurative bronchitis, severe hemorrhagic erosions, and late complications of the respiratory system including chronic bronchitis, bronchial wall thickening, interstitial lung disease, bronchiectasis, tracheobroncho malacia, air trapping and bronchiolitis, asthma, emphysema, strictures, and fibrosis.[1–3,5,7,14] Death may occur in the first few days to weeks following exposure, and has been reported to result from epithelial sloughing and airway obstruction.[4]

Because the overt effects of SM exposure may not be seen for up to 48 h, with some symptoms manifesting over days, other tests have been employed to help determine the extent of exposure. Testing urine for thiodiglycol, the primary metabolite of SM, is the most commonly measured fluid, but the metabolite can also be found and tested for in blood and blister fluid.[15] While these tests help to provide answers about the amount of exposure the victim has received, they take a number of hours to perform and do not directly correlate with the extent of local injury, particularly to vital organs such as the lungs. Methods to accurately detect potentially life-threatening airway mustard injury in the early stages following exposure are needed.

Optical coherence tomography (OCT) is a recently developed technology capable of providing real-time, noninvasive high-resolution (micron-level) imaging of tissues such as trachea and bronchi to depths of up to 3 mm below the tissue surface. During acute inhalation injury from agents such as SM, early changes in the epithelium, mucosa, and submucosa should be readily detectable by OCT.

Because SM continues to be a threat worldwide to both civilians and military personnel, we have developed an animal model of SM exposure using 2-chloroethylethylsulfide (CEES), also known as half-mustard, a monofunctional liquid derivative of sulfur mustard, and a noninvasive OCT method of detecting exposure injury in the airway. We propose that OCT may be an ideal technology for detecting and quantitatively assessing the degree of SM and CEES induced large airway injury from the earliest exposure to advanced stages. The ability to detect mustard induced airway injury at its earliest phases should facilitate more accurate triage, timely in-tervention, and better assessment of the effects of potential therapeutic interventions.

2 Methods

This study was approved by the University of California Irvine (UCI) Accreditation of Laboratory Animal Care (AAA-LAC) accredited Animal Research Committee (ARC) and the Department of Defense ARC in compliance with all state and federal animal welfare regulations. New Zealand white rabbits (N=14) (Western Oregon Rabbit Company, Philomath, Oregon) weighing 3 to 4.5 kg were used in this study. The animals were anesthetized with a 2:1 ratio of ketamine HCl (100 mg/ml) (Ketaject, Phoenix Pharmaceutical Incorporated, Saint Joseph, Missouri): xylazine (20 mg/ml) (Anased, Lloyed Laboratories, Shenendoah, Iowa), 0.75-cc/kg IM using a 23 gauge 5/8-in. needle. After the IM injection, a 23 gauge 1-in. catheter was placed in the marginal ear vein to administer IV maintenance anesthetic of a 1:1 mixture of ketamine:xylazine (10cc each of ketamine 100 mg/ml and xylazine 20 mg/ml) diluted to 55 ml in saline as a continuous infusion, at a rate of 0.17 ml/min. A dose of analgesic, Torbutrol 0.4-mg/kg SQ (Torbugesic-SA, Fort Dodge Animal Health, Fort Dodge, Iowa), was administered prior to intubation. The animals were orally intubated with a 3.5-mm cuffed endotracheal tube (14 cm in length) and mechanically ventilated (dual phase control respirator, model 613, Harvard Apparatus, Chicago, Illinois) at a respiratory rate of 32/ min and a tidal volume of 50 cc and FiO_2 of 100%. On completion of the experiment, the animals were euthanized with 1 cc of an intravenous injection of Eutha-6, administered through the marginal ear vein.

2.1 2-Choloroethyl Ethyl Sulfide Half-Mustard Administration

The animals enrolled in this study were placed on their right side, inside an approved fume hood. A pulse oximeter was attached to the forearm to monitor the pulse and SpO_2. The outer protective tubing of the OCT probe was tied to a PICC line (24 gauge × 30 cm, Becton Dickinson, Sandy, Utah) with O-silk at four places spaced about 4 cm apart. The probe combined with the PICC line was inserted through a Touey-Borst Y-adapter valve attached to the distal end of the endotracheal tube. The probe was then inserted through the valve and advanced down the endotracheal tube to a position 3 cm past the end of the tube to the distal tracheal region for imaging. A solution of 5-mg CEES dissolved in 0.5-ml phosphate buffered saline (PBS) was slowly injected through the PICC line, followed by a flush with 1cc of 0.9% NaCl.

The progression of injury was monitored over 8 h with intermittent imaging, with OCT images being captured every 15 min for up to 8 h postexposure.

2.2 Optical Coherence Tomography System and Probes

The OCT system used in this study contained a superluminescent diode source that delivered an output power of 10 mW at a central wavelength of 1310 nm with a full width at half maximum (FWHM) of 80 nm resulting in approximately 10-μm axial resolution, which resulted in approximately

15-μm axial and lateral resolution as delivered through the flexible fiber optic probe. The system has been previously described.[16–18] The focal distance of the gradient index (GRIN) lens was 2 mm, resulting in a focal depth optimum approximately 1 mm from the sheath wall. The probe was generally operated between approximately 1/2 to 1 mm from the tracheal surface, and we attempted to keep it from contacting the airway wall whenever possible. However, image quality was maintained at a range of distances, even in the contact mode, because of the low numerical aperture lens.

In the reference arm, a rapid-scanning optical delay line was used that employs a grating to control the phase and group delays separately, so that no phase modulation is generated when the group delay is scanned. The phase modulation was generated through an electro-optic phase modulator that produced a carrier frequency. The axial line scanning rate was 500 Hz, and the modulation frequency of the phase modulator was 500 kHz. Reflected beams from the two arms were recombined in the interferometer and detected on a photodetector. The detected optical interference fringe intensity signals were bandpass filtered at the carrier frequency. Resultant signals were then digitized with an analog-digital converter, which performed 12 bit at 5-MHz signal conversion and transferred information to a computer where the structural image was generated.

Flexible fiber optic OCT probes were constructed from single mode fiber (ThorLabs, Newton, New Jersey). The bare-ended fiber was attached to a 0.7-mm diam GRIN lens (NSG America, Irvine, California), using optical adhesive (Dymax Company, Torrington, Connecticut) under a microscope. A right angle light path was achieved using a 0.7-mm prism. The probe was placed in FEP tubing (17 gauge thin wall, Zeus, Orangeburg, South Carolina) for added fiber support. The outer diameter of the probe is approximately 2 mm.

A linear motor (Newport Instruments, Irvine, California) was used to drive the coated flexible fiber optic distally and proximally along the length of the probe within the sheath, moving the GRIN lens and prism imaging components within the sheath to obtain linear images along the long axis of the trachea and bronchi. Axial scans were obtained every 10 μm along the length of the probe during 16-mm-long scan sweeps. A 16-mm scan is obtained in 3.2 sec.

2.3 Brush Biopsy and Fluorescence Microscopy

Three of the animals in the experimental group underwent an endobronchial cytologic brush sampling of the tracheal wall through the endotracheal tube following the administration of CEES. The purpose of this was to observe cytoskeletal perturbation after administration of CEES, specifically disruption of tubulin microtubules and actin filaments. A premeasured 7.0-mm cytology brush (Harrell Bronchoscope Unsheathed Cytology Brush 7.0 mm, Conmed, Billerica, Massachusetts) was inserted down and just past the distal end of the endotracheal tube. The brush was moved proximally and distally with a sweep distance of approximately 2 cm, brushing a total of 4 to 5 times. The brush was then returned to the starting position just below the distal end of the endotracheal tube, and rotated 4 to 5 times in 360-deg revolutions. Once removed from the endotracheal tube, the brush was placed into a 15-mL centrifuge tube containing 1 mL sterile PBS and 1-μM DAPI. The tube and brush were shaken to release epithelial cells from the brush into the PBS. The end of the brush was clipped off and the tube was capped. Following this, the tube with brush end was vortexed 2 to 3 times for 1-sec pulses. Before the brush was removed from the tube, it was gently tapped against the side of the tube to remove any residual fluid containing cells. After the vortexing was complete, the cells obtained from the trachea were suspended in PBS and plated on glass coverslips. Cells were incubated at 37 °C for a 1-h period to allow cells to adhere to the coverslip. Cells were fixed with 4% paraformaldehyde/PBS and permeabilized in a 0.1% Triton X/2.5% fetal bovine serum blocking buffer. Subsequently, cells were stained for tubulin and actin using an antibeta tubulin—Cy3 conjugated antibody (Sigma) and phalloidin using Oregon green 488 (Invitrogen) during a 1-h incubation period. Cells were washed in triplicate following the incubation period. The brushings were collected immediately prior to sacrificing the animal, and the tracheas were collected for histology about 5-min postsacrifice. This procedure was performed on three animals, at 5-min, 30-min, and 3-h post-CEES instillation.

The fluorescence images were acquired using a Zeiss 200M (Zeiss, Thornwood, New York) inverted phase contrast/fluorescent microscope and a Zeiss 63×PH3 oil immersion apochromat objective lens (NA=1.4). The fluorescence excitation source used for imaging was the X-Cite 120 illumination system (EXFO Photonics Solutions, Incorporated, Ontario, Canada). Images were captured by a Hamamatsu Orca digital charge-coupled device (CCD) camera (Hamamatsu Corporation, Bridgewater, New Jersey). Exposure parameters, fluorescence filters, and light sources were controlled by the custom-coded Robolase software.[19] ImageJ software was used for image processing and analysis.

2.4 Sacrifice and Histology

Animals were sacrificed at the desired time points with 1 to 2 cc of Euthasol (350-mg pentobarbital sodium and 50 mg phenytoin sodium, Virbac Animal Health, Fort Worth, Texas) administered through the marginal ear vein, followed by 0.5cc of heparin flush. Following sacrifice, an interior neck dissection was performed to expose the trachea. A benchtop 635-nm laser source was used as an aiming beam (Thorlabs, Newton, New Jersey) to highlight the area imaged. Once this area was isolated, the trachea was excised and prepared for histology. The trachea was washed in saline and fixed in formalin.

3 Results

Notable tissue effects from CEES were observed earlier by OCT than previous studies had reported.[20,21] Marked epithelial and mucosal layer thickening became apparent very quickly in those animals that received CEES treatment (N=8), evident less than 15-min post exposure. The progression of injury continued to be observed over the 8 h of imaging (Fig. 1). Minimal to no thickening was observed in the control animals (N=3) (Fig. 2).

Histology specimens confirmed evidence of exposure to CEES (Fig. 3). The tracheas of the animals exposed to mustard exhibited large areas of mucosal ulceration and intraepithelial blisters. The submucosal vessels were dilated, congested, and contain thrombi. There was inflammation and
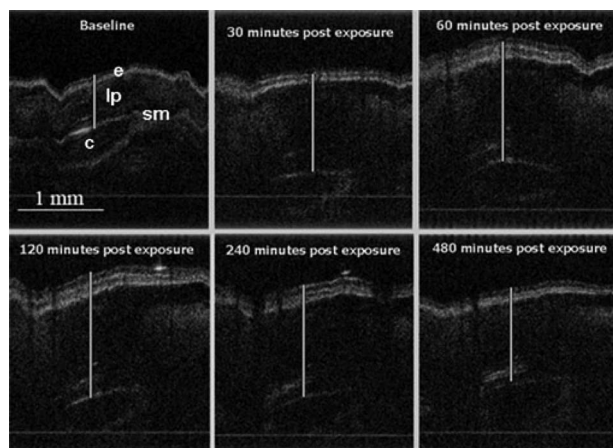
Fig. 1 OCT of a rabbit trachea exposed to CEES. Airway tissue region thickening can be seen throughout the duration of the experiment. Epithelium (e), cartilage (c), submucosal layers (sm), and lamina propria (lp) are easily visualized.

Fig. 2 OCT of a control animal at (a) 0 and (b) 360 min. Minimal thickening can be observed between the timepoints. Epithelium (e), cartilage (c), submucosal layers (sm), and lamina propria (lp) are easily visualized.

extensive hemorrhage in the wall of the bronchus. The control animals had preserved respiratory epithelium (Fig. 4). Areas of patchy and discrete ulcers were occasionally observed in control animal specimens. This was most likely due to intubation with a slightly larger than usual endotracheal tube which appears to have mildly abraded the walls of the trachea on insertion. In contrast to the mustard-exposed animals, the submucosal vessels in control animals were patent, and there was minimal evidence of hemorrhage and inflammation in the wall of the trachea.

The samples of tracheal cells obtained from the brush biopsies revealed damage to the tracheal surface from CEES exposure as well. Fluorescence microscopy of the control animals shows an abundance of actin within the cell body and a high concentration of ciliated structures at the periphery [Figs 5(a) and 5(b)]. The brush biopsies collected 5 min following exposure to CEES show a loss of actin and ciliated structures [Figs 5(c) and 5(d)]. The samples at 3-h post-CEES exposure did not reveal many additional changes in the concentration o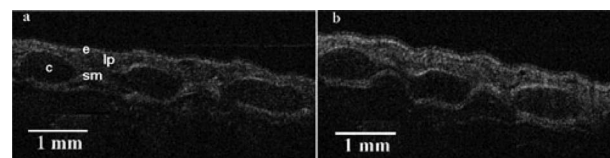f actin when compared to the 5-min samples. The most significant change was observed in the ciliated structures, where there was a large reduction in structure concentration [Figs 5(e) and 5(f)].

4 Discussion

Mustard gas exposure remains a major potential threat to military and civilian personnel. Lung injury, the most common lethal site of exposure, leads to acute tracheal, bronchial, and broncho–alveolar injury. Literature reports that the earliest clinical pulmonary affects begin to manifest at 4 to 6 h following exposure.[20,21] Lethal changes include sloughing of the mucosa with airway obstruction beginning to develop most commonly at 1 to 7 days postexposure. Difficulties in determining the presence as well as the extent of exposure severely limit optimal delivery of care to potentially exposed victims. Therefore, it is essential to develop quantitative, minimally invasive methods for detecting and assessing the extent of mustard-induced airway injury using new technologies such as OCT.

In this animal model of CEES airway injury, OCT images of a high quality were readily obtainable. The earliest OCT changes in the mucosa and submucosa region are apparent within minutes following exposure, in marked contrast to the reported 4 to 6 h earliest detectable changes by current clinical methodologies. The earliest changes appear to include edema and hyperemia,[22] with epithelial layer separation and hemorrhage developing over the next few hours. Increased airway soft tissue layer thickening and progression to fluid filled spaces and regions of sloughing are all readily apparent with continuous OCT monitoring. These are consistent with
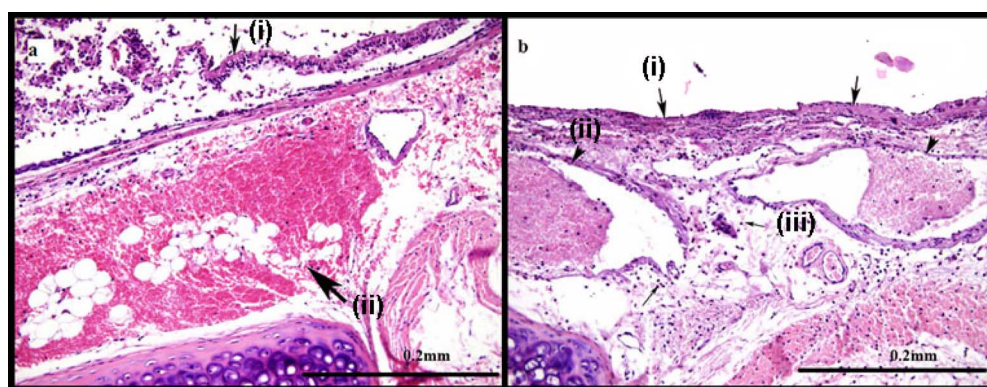

Fig. 3 Images from an animal with mustard exposure. (a) Intraepithelial blisters [small arrow (i)] and extensive hemorrhage in the wall of the trachea [large arrow (ii)] are visible using HE staining after exposure to CEES. (b) Diffuse mucosal ulceration [large arrows (i)], vascular thrombi [arrow heads (ii)] and inflammation [small arrows (iii)] are also visible in the histology sample.
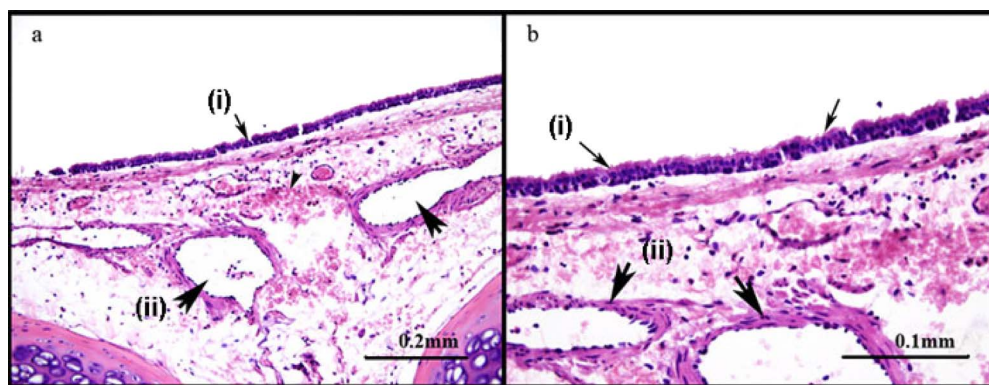
Fig. 4 (a) Control animal possesses preserved respiratory epithelium [small arrows (i)], normal submucosal vessels [large arrows (ii)] and minimal sub mucosal hemorrhage. (b) Control animal shows more detail of preserved structures at a higher magnification.

cellular changes seen in the brush biopsy specimens using cytoskeletal staining in our study, and consistent with the early changes some have reported in *in-vitro* culture model findings.[23] The extent of injury could potentially be quantitatively measured with this simple time-domain OCT system.

Tracheal brush cytologic sampling of the CEES injury obtained shortly after exposure revealed cytoskeletal changes occurring within minutes, leading to the changes in airway epithelial and mucosa regions visualized by OCT. Histopa-

Fig. 5 Actin and microtubule staining of control and CEES exposed rabbit tracheal epithelial cells (RTEC) show the degeneration of the cytoskeleton. (a) and (b) show an abundance of actin in green within the RTEC cell body, and microtubules in red that localize to the ciliated structures at the cell periphery. (c) and (d) show the cytoskeleton of RTEC cells 5 min following CEES exposure. A loss in actin signal within the cell body is observed as well as a decrease in the amount of ciliated structures at the periphery of the cell. (e) and (f) show the cytoskeleton of RTEC cells 3 h following CEES exposure. Similar to the 5-min exposed cells, a less intense actin signal is observed. At this time point, the largest changes were observed in the ciliated structures where the number of ciliated structures decreased substantially. Those structures that are present are significantly distorted, showing many irregular twists within the microtubule structures. (Color online only.)

thology at the time of sacrifice demonstrated separation and sloughing of the epithelial layer, mucosal and submucosal hemorrhage, and blistering.

The ability of OCT to detect the earliest changes from inhalation airway injury in a minimally invasive manner provides a new potential tool for improved diagnosis, assessment, and monitoring of mustard exposure. This study has demonstrated the feasibility of the concept in an animal model. Changes are apparent much earlier than previously detectable by other methods. The progression of injury over time can be observed. This should enable improved triage and resource allocation, facilitate clinical decision making, and should provide a method for assessing response to potential therapeutic agents in mustard injury. A wide range of potential agents have been proposed to ameliorate mustard-induced injury either prophylactically or in postexposure settings, including acetylcysteine, free radical scavengers such as superoxide dismutases, antioxidants including catalase, dimethyl sufoxide, organophosphates, sulfhydryl agents, neutrophil or complement depletion,[21,24–28] and for long-term complications with drugs such as steroids.[6] The ability to detect and quantitatively measure affects of these agents in real time throughout the evolution of the injury process could be an extremely valuable tool in determination of efficacy of such potential treatment agents.

Long-term airway sequelae following mustard injury are also a major medical issue. 40 to 50% of the more than 34,000 mustard-exposed victims from the Iran-Iraq war[9] and 95% of mustard-exposed patients in another study from Khorasan, Iran[2] have evidence of clinical lung disease, and lung complications are the most frequently occurring long-term complication.[9,14] 100% of cases of severely exposed victims had pulmonary bronchial wall thickening, and 80% of these patients had additional pulmonary abnormalities.[1] Long-term airway epithelial injury was seen in greater than 90% of patients an average of 14 years following exposure.[3] Airway strictures leading to respiratory death have occurred months to years after exposure and currently necessitate frequent invasive bronchoscopic procedures for monitoring.[5] OCT is capable of visualization of airway epithelia and mucosa, and we speculate that OCT may prove valuable in long-term airway sequelae diagnostics in the future. This technology may also
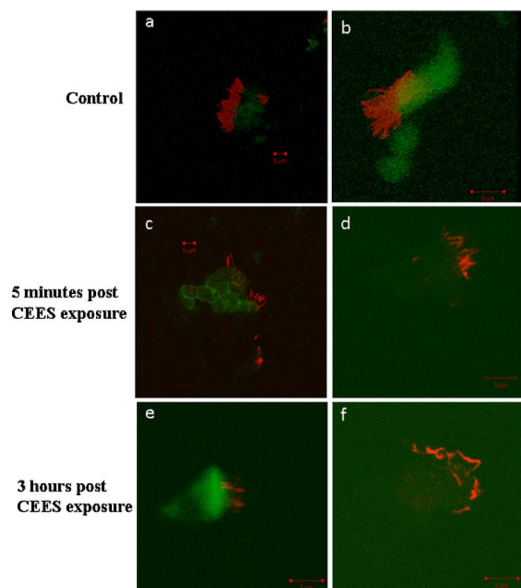
be useful in a wide range of other airway inhalation injury and toxic exposures.[16,17]

There are a number of limitations in this study. A single site of 2-D monitoring in the trachea was utilized in this study. In contrast to inhaled mustard gas exposure, liquid CEES exposure injury is focally concentrated in the areas where the CEES contacts the airway mucosa. Where the liquid does not contact the mucosa, the airway remains normal. Thus, the injury is heterogeneous. In animals where the OCT probe was inadvertently directed toward areas that were not directly exposed to CEES, changes were not seen. Regional inhomogeneities of injury following CEES exposure would be better evaluated by 3-D imaging of the airways to accurately describe the injury process. Ultrafast spectral-domain 3-D OCT airway imaging systems are being developed that will enable such imaging in the near future. Future studies should compare mustard gas exposure to CEES injury with these 3-D imaging systems.

In this study, we did not directly demonstrate that we can follow response to therapy, and we cannot differentiate the components of the histological changes occurring (blood, edema, hyperemia) other than detecting the onset of blistering and epithelial sloughing. Future developments with ultrahigh OCT resolution technologies may overcome these limitations. Furthermore, much more rapid imaging systems with broadband laser sources including frequency domain OCT, sweep source laser OCT, and MEMS-based probes will allow faster acquisition, enabling 3-D imaging, with higher resolution. Such capabilities should improve the accuracy of diagnosis, regional variability assessment, and ability to differentiate the pathologic events occurring during the evolution of the injury process.

From a practical standpoint, access to OCT may not be readily available at remote sites where mustard exposure may occur. However, this technology is fundamentally reducible to relatively inexpensive commercial devices that could be more widely accessible in the future.

5 Summary

This study demonstrates the feasibility of utilizing real-time minimally invasive OCT for high resolution detection and monitoring of mustard inhalation airway injury. The ability to detect very early injury changes may provide a tool for improved detection, triage, and therapeutic agent assessment. Future studies will be needed to determine the correlation between the acute injury changes seen in this model injury with later sequelae, survival, and prognosis. OCT technology may also have future applications in other forms of airway injury and toxic inhalation exposures.

References

1. M. H. Bagheri, S. K. Hosseini, S. H. Mostafavi, and S. A. Alavi, "High-resolution CT in chronic pulmonary changes after mustard gas exposure," *Acta Radiol.* **44**(3), 241–245 (2003).
2. M. Balali-Mood, M. Hefazi, M. Mahmoudi, E. Jalali, D. Attaran, M. Maleki, M. E. Razavi, G. Zare, A. Tabatabaee, and M. R. Jaafari, "Long-term complications of sulphur mustard poisoning in severely intoxicated Iranian veterans," *Fundam. Clin. Pharmacol.* **19**(6), 713–721 (2005).
3. J. Beheshti, E. J. Mark, H. M. Akbaei, J. Aslani, and M. Ghanei, "Mustard lung secrets: long term clinicopathological study following mustard gas exposure," *Pathol. Res. Pract.* **202**(10), 739–744 (2006).
4. W. Eisenmenger, G. Drasch, M. von Clarmann, E. Kretschmer, and G. Roider, "Clinical and morphological findings on mustard gas [bis(2-chloroethyl)sulfide] poisoning," *J. Forensic Sci.* **36**(6), 1688–1698 (1991).
5. L. Freitag, N. Firusian, G. Stamatis, and D. Greschuchna, "The role of bronchoscopy in pulmonary complications due to mustard gas inhalation," *Chest* **100**(5), 1436–1441 (1991).
6. M. Ghanei, A. R. Khalili, M. J. Arab, M. Mojtahedzadeh, J. Aslani, M. Lessan-Pezeshki, Y. Panahi, and F. Alaeddini, "Diagnostic and therapeutic value of short-term corticosteroid therapy in exacerbation of mustard gas-induced chronic bronchitis," *Basic Clin. Pharmacol. Toxicol.* **97**(5), 302–305 (2005).
7. M. Ghanei, M. Mokhtari, M. M. Mohammad, and J. Aslani, "Bronchiolitis obliterans following exposure to sulfur mustard: chest high resolution computed tomography," *Eur. J. Radiol.* **52**(2), 164–169 (2004).
8. M. Hefazi, D. Attaran, M. Mahmoudi, and M. Balali-Mood, "Late respiratory complications of mustard gas poisoning in Iranian veterans," *Inhalation Toxicol.* **17**(11), 587–592 (2005).
9. S. Khateri, M. Ghanei, S. Keshavarz, M. Soroush, and D. Haines, "Incidence of lung, eye, and skin lesions as late complications in 34,000 Iranians with wartime exposure to mustard agent," *J. Occup. Environ. Med.* **45**(11), 1136–1143 (2003).
10. R. N. Saladi, E. Smith, and A. N. Persaud, "Mustard: a potential agent of chemical warfare and terrorism," *Clin. Exp. Dermatol.* **31**(1), 1–5 (2006).
11. M. J. Geraci, "Mustard gas: imminent danger or eminent threat?," *Ann. Pharmacother.* **42**(2), 237–246 (2008).
12. M. I. Dabrowska, L. L. Becks, J. L. Lelli, Jr., M. G. Levee, and D. B. Hinshaw, "Sulfur mustard induces apoptosis and necrosis in endothelial cells," *Toxicol. Appl. Pharmacol.* **141**(2), 568–583 (1996).
13. M. A. Mol, R. M. van den Berg, and H. P. Benschop, "Proteomic assessment of sulfur mustard-induced protein adducts and other protein modifications in human epidermal keratinocytes," *Toxicol. Appl. Pharmacol.* **230**(1), 97–108 (2008).
14. M. Ghanei, F. A. Moqadam, M. M. Mohammad, and J. Aslani, "Tracheobronchomalacia and air trapping after mustard gas exposure," *Am. J. Respir. Crit. Care Med.* **173**(3), 304–309 (2006).
15. J. Newmark, J. M. Langer, B. Capacio, J. Barr, and R. G. McIntosh, "Liquid sulfur mustard exposure," *Mil. Med.* **172**(2), 196–198 (2007).
16. M. Brenner, K. Kreuter, J. Ju, S. Mahon, L. Tseng, D. Mukai, T. Burney, S. Guo, J. Su, A. Tran, A. Batchinsky, L. C. Cancio, N. Narula, and Z. Chen, "In vivo optical coherence tomography detection of differences in regional large airway smoke inhalation induced injury in a rabbit model," *J. Biomed. Opt.* **13**(3), 034001 (2008).
17. M. Brenner, K. Kreuter, D. Mukai, T. Burney, S. Guo, J. Su, S. Mahon, A. Tran, L. Tseng, J. Ju, and Z. Chen, "Detection of acute smoke-induced airway injury in a New Zealand white rabbit model using optical coherence tomography," *J. Biomed. Opt.* **12**(5), 051701 (2007).
18. N. M. Hanna, W. Waite, K. Taylor, W. G. Jung, D. Mukai, E. Matheny, K. Kreuter, P. Wilder-Smith, M. Brenner, and Z. Chen, "Feasibility of three-dimensional optical coherence tomography and optical Doppler tomography of malignancy in hamster cheek pouches," *Photomed. Laser Surg.* **24**(3), 402–409 (2006).
19. E. L. Botvinick and M. W. Berns, "Internet-based robotic laser scissors and tweezers microscopy," *Microsc. Res. Tech.* **68**(2), 65–74 (2005).
20. J. P. Petrali and S. Oglesby-Megee, "Toxicity of mustard gas skin lesions," *Microsc. Res. Tech.* **37**(3), 221–228 (1997).
21. S. D. McClintock, G. O. Till, M. G. Smith, and P. A. Ward, "Protection from half-mustard-gas-induced acute lung injury in the rat," *J. Appl. Toxicol.* **22**(4), 257–262 (2002).
22. A. Emad and G. R. Rezaian, "Immunoglobulins and cellular constituents of the BAL fluid of patients with sulfur mustard gas-induced pulmonary fibrosis," *Chest* **115**(5), 1346–1351 (1999).

23. J. H. Calvet, J. P. Gascard, S. Delamanche, and C. Brink, "Airway epithelial damage and release of inflammatory mediators in human lung parenchyma after sulfur mustard exposure," *Hum. Exp. Toxicol.* **18**(2), 77–81 (1999).

24. D. R. Anderson, S. L. Byers, and K. R. Vesely, "Treatment of sulfur mustard (HD)-induced lung injury," *J. Appl. Toxicol.* **20**(Suppl 1), S129–132 (2000).

25. A. Eldad, P. Ben Meir, S. Breiterman, M. Chaouat, A. Shafran, and H. Ben-Bassat, "Superoxide dismutase (SOD) for mustard gas burns," *Burns* **24**(2), 114–119 (1998).

26. S. D. McClintock, L. M. Hoesel, S. K. Das, G. O. Till, T. Neff, R. G. Kunkel, M. G. Smith, and P. A. Ward, "Attenuation of half sulfur mustard gas-induced acute lung injury in rats," *J. Appl. Toxicol.* **26**(2), 126–131 (2006).

27. R. Vijayaraghavan, P. Kumar, U. Joshi, S. K. Raza, P. V. Lakshmana Rao, R. C. Malhotra, and D. K. Jaiswal, "Prophylactic efficacy of amifostine and its analogues against sulphur mustard toxicity," *Toxicology* **163**(2-3), 83–91 (2001).

28. U. Wormser, "Toxicology of mustard gas," *Trends Pharmacol. Sci.* **12**(4), 164–167 (1991).